



**This is a pre- or post-print of an article published in  
Franzen, L., Selzer, D., Fluhr, J.W., Schaefer, U.F.,  
Windbergs, M.  
Towards drug quantification in human skin with confocal  
Raman microscopy  
(2013) European Journal of Pharmaceutics and  
Biopharmaceutics, 84 (2), pp. 437-444.**

# Towards drug quantification in human skin with confocal Raman microscopy

Lutz Franzen<sup>a</sup>, Dominik Selzer<sup>a</sup>, Joachim Fluhr<sup>b</sup>, Ulrich F. Schaefer<sup>a</sup>, Maike Windbergs<sup>a,c,d</sup>

<sup>a</sup>*Biopharmacy and Pharmaceutical Technology, Saarland University, Saarbruecken, Germany*

<sup>b</sup>*Department of Dermatology, Venerology and Allergology, Charite, Berlin, Germany*

<sup>c</sup>*Pharmbiotec GmbH, Saarbruecken, Germany*

<sup>d</sup>*Helmholtz-Institute for Pharmaceutical Research Saarland, Saarbruecken, Germany*

## Corresponding author:

Dr. Maike Windbergs

Department for Biopharmaceutics and Pharmaceutical Technology

Saarland University, Campus A4.1

66123 Saarbruecken

m.windbergs@mx.uni-saarland.de;

Phone: +49 681 302 2358

Fax: +49 681 302 4677

<sup>a, c, d</sup> Saarland University, Campus A4.1

66123 Saarbruecken

Germany

lutz.franzen@mx.uni-saarland.de

d.selzer@mx.uni-saarland.de

ufs@mx.uni-saarland.de

<sup>b</sup> Luisenstr.2

10117 Berlin

Germany

jochim.fluhr@charite.de

## **Abstract**

Understanding the penetration behavior of drugs into human skin is a prerequisite for the rational development and evaluation of effective dermal drug delivery.

The general procedure for the acquisition of quantitative drug penetration profiles in human skin is performed by sequential segmentation and extraction. Unfortunately, this technique is destructive, laborious and lacks spatial resolution. Confocal Raman microscopy bares the potential of a chemically selective, label free and non-destructive analysis. However, the acquisition of quantitative drug depth profiles within skin by Raman microscopy is impeded by imponderable signal attenuation inside the tissue.

In this study, we present a chemical semi-solid matrix system simulating the optical properties of human skin. This system serves as a skin surrogate for investigation of Raman signal attenuation under controlled conditions. Caffeine was homogeneously incorporated within the skin surrogate and Raman intensity depth profiles were acquired. A mathematical algorithm describing the Raman signal attenuation within the surrogate was derived from these profiles. Human skin samples were incubated with caffeine and Raman intensity depth profiles were similarly acquired. The surrogate algorithm was successfully applied to correct the drug profiles in human skin for signal attenuation. For the first time, a mathematical algorithm was established which allows correction of Raman signal attenuation in human skin, thus facilitating reliable drug quantification in human skin by confocal Raman spectroscopy.

**Keywords:** confocal Raman microscopy, human skin, quantitative depth profiling, dermal drug delivery, skin surrogate, Raman signal attenuation

## Introduction

The analysis of dermal drug absorption is essential for rational development of novel drug delivery options via the skin. As composition and barrier function of animal skin differ from human skin, the transferability of absorption data from animal testing to human skin is exacerbated [1]. Thus, for appropriate *in vitro* testing of dermal drug delivery, excised human skin is the gold standard specimen.

Human skin comprises a complex assembly of different layers with varying composition. The stratum corneum as the outermost skin layer represents the main barrier. Therefore, most *in vitro* penetration and permeation studies focus on this particular layer. According to the brick-mortar model, the stratum corneum consist of hydrophilic corneocytes surrounded by an extracellular lipid matrix [2]. Most substances enter the skin via an extracellular pathway, diffusing along this lipid matrix. The analysis of penetration processes in the different skin layers is a complex and laborious procedure which requires destructive segmentation as well as extraction [3]. Furthermore, the analytical determination lacks spatial resolution.

Recently, biophysical techniques like confocal laser scanning microscopy [4] or two photon microscopy [5, 6] have been proven to provide spatially resolved information about kinetics and depth of dermal penetration and molecular interaction with the skin. However, quantification of drug penetration by two photon microscopy is limited to autofluorescent drug compounds in the absence of dyes or labels. Linking drugs with dyes or labels potentially introduces changes in substance physicochemical properties like lipophilicity or molecular weight which impair reliable transferability of the data. Unlike the former mentioned techniques, vibrational spectroscopy provides direct molecular information of the sample without labelling. For instance, infrared (IR) spectroscopy was successfully used to track lipids within the skin [7]. Unfortunately, the use of this technique is limited by its sensitivity to water.

In this context, Raman spectroscopy as a complementary analytical technique to IR spectroscopy bears a lot of potential for the analysis of skin. In contrast to IR, Raman spectroscopy is not constraint by the presence of water. By detecting the frequency shift of scattered laser light after irradiating a sample, chemically selective information of the sample composition is acquired. Furthermore, combining Raman spectroscopy with a confocal microscope provides spatially resolved analysis of the sample. Thus, confocal Raman microscopy is a promising analytical approach for label free and non destructive follow-up of substances within human skin.

Confocal Raman spectroscopy has already been applied for analysis of skin hydration status [8], the effect of penetration enhancers [9] and the epidermal antioxidative potential [10, 11] of skin. *In vitro* follow-up studies of metronidazole [12] and phospholipids [13] indicated the potential of confocal Raman microscopy for penetration experiments.

Recently, several authors described mathematical models to correct depth determination uncertainties of confocal Raman microscopy in polymer films [14-16]. Previous studies used these models to improve accuracy of confocal depth determination in skin [17]. Determination of the exact depth of the focal plane inside human skin allows the accurate acquisition of qualitative drug penetration follow-up profiles.

However, for rational development and *in vitro* testing of novel dermal drug delivery systems quantitative analysis of drug penetration processes is mandatory. Unfortunately, so far drug quantification within skin based on Raman microscopy is exacerbated by Raman signal attenuation, as with increasing depth a decrease in Raman signal intensity distorts reliable drug quantification. One approach to overcome the influence of Raman signal attenuation in skin was already performed by relating the intensity of a drug Raman peak to the intensity of a skin derived Raman peak [12, 18]. Unfortunately, potential inhomogenities due to the complex skin structure cannot be taken into consideration with this relative method. For reliable quantification of substances inside human skin by Raman microscopy the exact extent of Raman signal attenuation has to be determined. As Raman microscopy offers unique possibilities for non-destructive and chemically selective analysis of substances in human skin, there is a strong need to overcome the analytical pitfalls exacerbating a reliable quantification of drugs in skin samples.

In this study, we present a novel approach to quantify Raman signal attenuation in human skin. We successfully developed a simplified and reproducible surrogate system simulating the optical properties of human stratum corneum. A comprehensive physical characterization comprising spectroscopic as well as thermoanalytical methods was performed on the skin surrogate as well as on its single components followed by a comparison to excised human skin samples. Caffeine was homogeneously incorporated within the skin surrogate and Raman depth profiles of caffeine were acquired. To address the issue of Raman signal attenuation, these profiles were mathematically fitted and a correction algorithm was

derived. Furthermore, excised human skin samples were incubated with caffeine and Raman intensity depth profiles were acquired. Using the surrogate algorithm, these human skin intensity depth profiles were finally corrected for Raman signal attenuation.

## **Materials and methods**

### **Skin surrogate fabrication**

The main chemical components of human stratum corneum were used to create a suitable skin surrogate, namely keratin as the main protein component, purified water and a specific lipid mixture (Table 1). The lipid mixture was based on the work of Jaeckle et al [19] and contains fatty acids, cholesterol and triglycerides in predefined ratios.

Keratin, extracted from rabbit fur (Chemos GmbH, Regenstaufen, Germany) and purified water were mixed in a melamin bowl by dropwise adding water to the keratin powder. The fatty acids myristinic acid (Edenor C 14®), palmitic acid (Edenor C 16®), stearic acid (Edenor C 18®), oleic acid (Edenor Ti05®) and linolic acid (Edenor SB05®), provided by Cognis Oleochemicals GmbH (Duesseldorf, Germany) were mixed and molten in a metal bowl at 75 °C forming a clear liquid and stirred during cooling down to room temperature. This mixture is referred to as 'fatty acids' in the text. Triglycerides (Witepsol H5®, Sasol, Hamburg, Germany) and cholesterol (Sigma-Aldrich, Steinheim, Germany) were added and the procedure was repeated as described. The cold lipid mixture was added to the keratin in water and finally homogenised. First approaches to form a homogeneous matrix involved gentle physical mixing of the components in a melamin bowl leading to inhomogeneous distribution of hydrophilic and lipophilic compounds and the incorporation of air bubbles. Further processing by means of a porphyrisator improved homogeneity but multiplied the air contribution, resulting in a foamy consistence.

The optimised fabrication process involves premixing in a melamin bowl and final homogenisation using a three-roll-mill. The appearance of the final product was a creamy matrix of bright brown colour. The refractive index of the skin surrogate was determined using a Abbe-refractometer. The final skin surrogate was stored at room temperature in a scintillation vial sealed with parafilm.

### **Incorporation of caffeine**

Micronized caffeine (Sigma-Aldrich, Steinheim, Germany) as a model drug was incorporated in the surrogate by adding the powdered substance to the keratin water mixture. The subsequent fabrication of the skin surrogate follows the protocol as described above. A caffeine concentration of 30 mg caffeine per 1 g surrogate was used as reported for penetration experiments in human skin [20]. This concentration could be detected by Raman microscopy without any constraints. To verify the homogenous distribution of caffeine, the surrogate is spread on a glass slide and at least six single spectra are recorded at random positions on the surrogate surface.

### **Human skin preparation**

Human skin was obtained from plastic surgery of female Caucasians (Department of Plastic and Hand Surgery, Caritaskrankenhaus, Lebach, Germany). Only abdominal skin was used. After excision the stratum corneum was cleaned with purified water and the fatty tissue was removed with a scalpel. The skin was stored in impermeable polyethylene bags at -26 °C. For stratum corneum isolation the protocol of Kligman et al [21] was followed. First, punches of 25 mm in diameter were taken from the frozen skin and thawed to room temperature on a filter paper soaked with phosphate-buffered saline (composed of 0.2 g potassium chloride, 8.0 g sodium chloride, 1.44 g disodium hydrogen phosphate dehydrate and 0.2 g potassium dihydrogen phosphate in 1 l of purified water). To separate the full-thickness skin in dermis and epidermis, the thawed sheets were immersed in 60 °C warm purified water for 90 s. Subsequently, the epidermis was peeled off using forceps. The dermis was disposed and the heat separated epidermis was transferred into a petri dish. To separate stratum corneum and epidermis, the sheets were incubated in 0.15 % (m/m) solution of trypsin in phosphate-buffered saline at 37 °C. After 24 h the remnants of viable epidermis were removed in purified water and the remaining stratum corneum sheets were blotted dry between two filter papers using a pressure roll. Placed on flat Teflon sheets the stratum corneum was freeze dried (Martin Christ Gefriertrocknungsanlagen GmbH, Osterode, Germany). The freeze drying process took at least 48 h and the crimp stratum corneum sheets were stored in a desiccator until further analysis.

### **Drug incubation experiments**

For drug incubation experiments the heat separated epidermis was incubated in a petri dish filled with caffeine solution (12.5 mg/ml) in phosphate-buffer for 12 h. After incubation, the skin was patted dry and analysed. For Raman measurements the skin was fixed on glass slides covered with adhesive aluminium foil. All measurements were performed at controlled temperature and humidity conditions (21 °C / 30-40 % rh).

### **Differential scanning calorimetry (DSC)**

Differential scanning calorimetry was used to study thermal characteristics of the surrogate and its single components. Samples of 2-3 mg were sealed in hermetic aluminium pans (Hermetic Pans, TA Instruments, USA). After equilibration for 2 min at 20 °C, temperature ramps in the range of 20-160 °C were performed with a heating rate of 10 °C/min (DSC Q100, TA Instruments, USA). For stability testing, the freshly prepared surrogate was sealed in hermetic pans and stored at room temperature (21 °C) for one or five days, respectively.

### **Confocal Raman microscopy**

For Raman analysis the surrogate was filled in silicon rings fixed on glass slides. This procedure results in a reproducible surrogate layer of 2 mm in thickness providing a plane upper surface suitable for single spectra and depth scan acquisition. Raman spectra were recorded using a confocal Raman microscope (alpha300R+, WITec GmbH, Ulm, Germany). The excitation source was a diode laser with a wavelength of 785 nm adjusted to a power of 25 mW on the sample surface. Single spectra were recorded using a 50x objective (Epiplan Neofluar, Zeiss, Germany) with a numeric aperture of 0.8. For z-line-scans the corresponding long distance objective (N.A. 0.55) was used. A confocal pinhole of 100 µm rejected signals from out-of-focus regions. Raman spectra were recorded in the range of 400-1780 cm<sup>-1</sup> with a spectral resolution of 4 cm<sup>-1</sup> and 10 seconds acquisition time with 10 accumulations. For depth profiling spectra were collected in 2 µm steps with 3 accumulations. All spectra were background subtracted and normalised to the most intense peak at 1430-1480 cm<sup>-1</sup> representing ν(C-H) vibration using WITec Project Plus software (WITec GmbH, Ulm, Germany).

### **Infrared-Spectroscopy (IR)**

Infrared spectroscopy analysis was performed with an attenuated total reflectance (ATR) unit (Spectrometer 400 ATR-IR, Perkin Elmer, USA). Spectra were recorded in the range of 650-4000  $\text{cm}^{-1}$  with 10 accumulations.

## **Results and discussion**

### **Skin surrogate fabrication**

The development of an artificial skin surrogate is based on the idea to establish a reproducible system simulating the optical properties of human stratum corneum. The surrogate composition is based on the chemical composition of human stratum corneum. Human stratum corneum consists of keratin as the main structure-forming protein and the intercellular lipid bilayers comprising fatty acids, triglycerides, cholesterol, ceramides and sterolesters (Table 2) [22-25].

Based on this information, a simplified composition of the main stratum corneum components is chosen (Table 1). The use of other components like ceramides appears to be unessential to achieve optical similarity. Homogeneity of the skin surrogate is non destructively verified by Raman spectroscopy.

### **Physical characterisation and stability testing**

To assure stability and reproducibility of the surrogate system, a comprehensive physical characterization of single components and the final surrogate is performed comprising thermoanalytical as well as spectroscopic methods. Furthermore, stability testing is conducted to monitor potential changes upon storage.

DSC thermograms of the single components and the surrogate are recorded (Figure 1 A). The lipid components (fatty acids, cholesterol and triglycerides) exhibit clear endothermic peaks, representing the respective melting processes. The denaturation of keratin is slightly visible around 110 °C, corresponding well with literature [26, 27]. The skin surrogate shows one endothermic peak around 35 °C, representing triglycerides and fatty acid melting. No additional peaks indicating transformations during fabrication can be observed.

As lipids are prone to undergo polymorphic transitions upon storage [28] the surrogate is analysed in terms of physical stability. A certain amount of skin surrogate is transferred to hermetically sealed DSC pans and thermoanalysis is performed directly after fabrication and after defined storage intervals in room conditions. The lipid melting endotherm around 35° C depicts a slim shoulder directly after fabrication indicating transitional lipid formations which disappears after one day (Figure 1 B) [29]. No further changes are observed up to five days after production. Based on these results all studies are carried out 24 h after surrogate fabrication, to assure the absence of lipid transformations during experiments.

### **Raman microscopy analysis**

As a basis for depth profiling, Raman analysis is performed on the single components as well as on the skin surrogate (Figure 2 A). The surrogate spectrum reflects the vibrational information of the single components without the appearance of any additional peaks or shifts. The most intense peak is localised at 1430-1480 cm<sup>-1</sup> representing  $\nu(\text{C-H})$  vibration as expected [30]. In a second step, the spectral information of the individual components is summed up to form a virtual surrogate spectrum. Based on the exact predefined ratios of the components in the skin surrogate, the single component spectra are combined by Equation 1 to form a virtual spectrum of the ideal, homogeneous mixture without any interactions.

$$\text{FA} * 0.114 + \text{TG} * 0.093 + \text{Chol} * 0.093 + \text{K/W} * 0.7 \quad (\text{Equation 1})$$

(FA = fatty acids, TG = triglycerides, Chol = cholesterol, K/W = keratin/water)

The virtual spectrum perfectly reflects the original skin surrogate spectrum without any shifted or additional peaks (Figure 2 B). Thus, the fabrication procedure does not affect the chemical structure and physical behaviour of the individual components. Furthermore, there is no hint for any interactions of the individual components.

### **Comparison of skin surrogate and human skin**

As the skin surrogate is supposed to serve as a model system to analyse Raman signal attenuation in human skin, the essential optical properties of the surrogate have to coincide with human skin.

As one of the main optical properties, the refractive index of the skin surrogate is determined using an Abbe-refractometer. The result of 1.48 (n=5) corresponds well

with the refractive index of human stratum corneum (1.51) [31]. Furthermore, IR and Raman spectroscopy were used as complementary techniques to compare isolated human stratum corneum and skin surrogate with each other (Figure 3). With respect to its simplified composition, the surrogate successfully mimics the spectroscopic properties of human stratum corneum. The Raman spectra of the surrogate represent the bands of the major components of human stratum corneum (Figure 3 A), explicitly the amid I stretch band at  $1650\text{ cm}^{-1}$  and the fatty acid C-C chains stretch at  $1125\text{ cm}^{-1}$  [30]. The Raman peak at  $1003\text{ cm}^{-1}$  is less pronounced in the surrogate due to overlapping of aromatic amino acid bands with the urea band in human skin, as urea is not included in the surrogate composition.

IR spectroscopy cannot detect any differences between stratum corneum and the skin surrogate except for peak broadening caused by higher water content in the skin surrogate (Figure 3 B).

The surrogate closely mimics the optical properties of human skin, which is an important prerequisite for simulating and evaluating Raman signal attenuation in human skin.

### **Incorporation of a model drug**

For a comprehensive investigation and quantification of Raman signal attenuation of drugs in skin, the surrogate needs to be homogeneously loaded with a drug, thus providing a controlled system with constant drug concentration at each point. Caffeine as a model drug is homogeneously distributed within the surrogate system. The comparison of Raman spectra of pure surrogate, a saturated aqueous caffeine solution and caffeine-loaded surrogate demonstrates the detectability of caffeine inside the skin surrogate (Figure 4 A). The spectrum of the caffeine loaded surrogate shows neither any additional peaks nor wavelength shifts of existing peaks. This indicates that caffeine remains chemically intact and causes no interactions with surrogate components.

Heat-separated epidermis (HSE), a standard skin sample for drug penetration testing, is used as specimen for comparison with the drug loaded surrogate. Incorporation of the drug into the skin sample is performed in a bath of caffeine solution. Thus, exclusive skin penetration via the stratum corneum as performed in a Franz cell experiment is avoided and the drug can diffuse into the skin sample from all sides. Raman spectra of freshly prepared HSE, caffeine solution and drug-loaded

HSE were acquired and compared to each other (Figure 4 B). No additional peaks or wavelength shifts of existing peaks can be observed. The main peaks representing caffeine are identified at  $553\text{ cm}^{-1}$  (deformation  $\delta(\text{O}=\text{C}-\text{N})$ ) and  $1337\text{ cm}^{-1}$  (stretch  $\nu(\text{CN})$ ) [32].

To verify a homogenous distribution of caffeine within the skin surrogate, three different batches of surrogate are analysed by confocal Raman microscopy. Figure 4 C depicts three representative spectra for each surrogate batch. The normalized peak intensities of the peak representing caffeine range from  $33.1\% \pm 3.2\%$  to  $29.7\% \pm 1.1\%$  ( $n = 6$ ) for the individual batches (Figure 4 D). Comparison of the mean peak intensities of three surrogate batches revealed no statistical difference. This proves reproducible and homogeneous concentrations of caffeine inside the surrogate.

### **Drug depth profiling**

For a profound investigation of Raman signal attenuation inside the skin, drug intensity depth profiles are acquired in the surrogate as well as in HSE samples. For this purpose, the intensity of the Raman signal representing caffeine in the wave number range of  $550\text{-}560\text{ cm}^{-1}$  is monitored. This region is chosen because it provided a clear signal even in deeper layers with higher ambient noise. Due to the subsistence of some small air bubbles in the skin surrogate, causing low signal intensities at certain depth points, the intensity depth profiles of the skin surrogate are smoothed.

Figure 5 depicts the caffeine intensity depth profiles in skin surrogate samples (A) and HSE samples of two different skin donors (B, C). Each profile exhibits a similar shape, consisting of a steep Raman intensity increase followed by a maximum and terminating in a levelled intensity decrease. The half maximum of the increase represents the depth where the measurement spot entered half way into the specimen [17]. Therefore, this depth is determined to be the sample surface. The peak maximum itself indicates that the measurement spot entered the sample completely, since Raman scattering is detected within the whole spot volume.

For the skin surrogate, the caffeine concentration is known to be constant at each depth due to homogeneous drug distribution inside the sample. Since Raman peak intensity is directly related to caffeine concentration, the Raman intensity in the surrogate is supposed to be constant at each point. Thus, a plateau at maximum

Raman intensity is expected when the measurement spot entered the sample completely, rather than the observed levelled decrease. Therefore, the detected Raman signal attenuation is exclusively caused by intensity damping in the sample. To quantify the extent of attenuation, the decrease of the curve is mathematically fitted.

### **Development of a correction algorithm for Raman signal attenuation**

One aim of the study is to develop a mathematical algorithm which allows to correct Raman intensity depth profiles for signal attenuation within the surrogate. Based on this algorithm drug concentration profiles with a direct correlation of Raman intensity changes and drug concentration changes shall be realized. In a further step, this algorithm is meant to be transferred to skin samples for correction of Raman depth profiles.

Based on the drug intensity depth profiles of three different skin surrogates a mean curve is calculated. In a next step, the decrease of this curve is fitted by an exponential function (Equation 2). Exponential fitting is chosen because it is well known that the intensity of electromagnetic waves undergo an exponential decay while penetrating an opaque medium. To avoid overfitting a simple exponential relationship as presented in Equation 2 is applied. Least-square regression with constraint  $D(0) = 1$  is applied to mathematically describe the decrease of the curve, with  $x$  being the depth along the  $z$ -axis and  $x = 0$  being the skin surrogate surface (Equation 3). The residual standard error is 0.04848 and the variables  $a$  and  $b$  are significantly different from zero with  $p < 0.001$ .

$$D(x) = a * \exp\left(-\frac{x}{b}\right) + (1 - a) \quad \text{(Equation 2)}$$

$$D(x) = 0.9997 * \exp\left(-\frac{x}{15.7581}\right) + (1 - 0.9997) \quad \text{(Equation 3)}$$

Equation 3 exhibits a representative mathematical description of the drug Raman signal intensity attenuation within the skin surrogate. Figure 6 displays the mean drug intensity depth profile and the corresponding fit by Equation 3. Apart from three single data points within the steepest decrease of the profile, the fit accurately describes the recorded data points. To obtain caffeine intensity depth profiles based on a direct correlation of Raman signal intensity and caffeine concentration in the surrogate, the attenuation based intensity decrease has to be mathematically corrected.

Using the attenuation function (Equation 3) a signal re-attenuating algorithm is derived with  $f(x)$  representing the detected Raman intensity at depth  $x$  and  $R(x)$  representing the corrected signal.

$$R(x) = f(x) + 1 - (0.9997 * \exp\left(-\frac{x}{15.7581}\right) + (1 - 0.9997))$$

(Equation 4)

As the skin surrogate simulates the optical properties of human stratum corneum, the re-attenuation algorithm is supposed to correct drug intensity profiles in human skin samples.

For a proof of concept, the re-attenuation algorithm is used to recalculate caffeine intensity depth profiles in HSE samples. Figure 7 shows mean drug intensity depth profiles of two different skin donors based on raw spectral data without any correction (solid line) and after processing the data with the re-attenuation algorithm (dashed line). After correction, the drug intensity depth profiles exhibit a nearly constant Raman intensity, which is directly related to the drug concentration within the whole skin sample. A slight deviance in the first part of the corrected profile is based on a less accurate fit in the steep part of the profile as discussed above. Incubating the skin samples in caffeine solution bypasses the stratum corneum barrier function and facilitates complete soaking with drug solution. Assuming that the caffeine concentration is constant in each depth in the HSE, a calculated constant intensity of the caffeine related Raman peak over depth in HSE is plausible. These results indicate the suitability of the correction algorithm to correct intensity depth profiles for Raman signal attenuation. So far, most studies relied on a relative method to deal with Raman signal attenuation. By applying this method, the intensity of a drug representing Raman peak is related to a skin derived Raman peak [12, 18]. Inconsistencies in Raman peak intensity due to inhomogeneities in skin composition are potentially causing uncertainties in depth profiling. Against this background, our novel approach to quantify Raman signal attenuation in a chemical skin surrogate with similar optical properties as skin and to generate a mathematical algorithm for correction of attenuation within skin samples bares many advantages. This approach potentially allows direct quantification of drug in skin tissue solely based on Raman peak intensities. Furthermore, the influence of skin inhomogeneities on concentration depth profiles is reduced. On the contrary to the existing qualitative and semi-quantitative studies, this facilitates the acquisition of quantitative concentration depth profiles [9, 12]. However, future studies will investigate the applicability of the

developed algorithm on a larger set of different drug depth profiles including a comparison of Raman spectroscopy results and established standard techniques for the acquisition of drug depth profiles.

### **Conclusion**

An artificial skin surrogate simulating the optical properties of human skin is successfully developed. Evaluation of the skin surrogate by comprehensive physical characterization with thermal and vibrational spectroscopy techniques proves reproducibility and stability of the system. A mathematical function for the description of Raman signal attenuation in the skin surrogate is derived based on an incubation study with a homogeneously distributed model drug and is applied to approximate drug intensity depth profiles in human skin. This novel mathematical approach serves as a first step towards a reliable acquisition of quantitative drug concentration profiles by confocal Raman microscopy.

### **Acknowledgements**

The Authors would like to thank K.-H. Kostka from Caritaskrankenhaus Lebach for providing freshly excised skin, D. Neumann from Scientific Consilience and T. Hahn for the fruitful discussions.

## References

- [1] F.P. Schmook, J.G. Meingassner, A. Billich, Comparison of human skin or epidermis models with human and animal skin in in-vitro percutaneous absorption, *Int J Pharm*, 215 (2001) 51-56.
- [2] P.M. Elias, Epidermal Lipids, Barrier Function, and Desquamation, *J Invest Dermatol*, 80 (1983) S44-S49.
- [3] H. Wagner, K.H. Kostka, W. Adelhardt, U.F. Schaefer, Effects of various vehicles on the penetration of flufenamic acid into human skin, *Eur J Pharm Biopharm*, 58 (2004) 121-129.
- [4] Y.Y. Grams, L. Whitehead, P. Cornwell, J.A. Bouwstra, Time and depth resolved visualisation of the diffusion of a lipophilic dye into the hair follicle of fresh unfixed human scalp skin, *J Control Release*, 98 (2004) 367-378.
- [5] B. Yu, K.H. Kim, P.T.C. So, D. Blankschtein, R. Langer, Visualization of oleic acid-induced transdermal diffusion pathways using two-photon fluorescence microscopy, *J Invest Dermatol*, 120 (2003) 448-455.
- [6] M.S. Roberts, Y. Dancik, T.W. Prow, C.A. Thorling, L.L. Lin, J.E. Grice, T.A. Robertson, K. Konig, W. Becker, Non-invasive imaging of skin physiology and percutaneous penetration using fluorescence spectral and lifetime imaging with multiphoton and confocal microscopy, *Eur J Pharm Biopharm*, 77 (2011) 469-488.
- [7] C.H. Xiao, D.J. Moore, C.R. Flach, R. Mendelsohn, Permeation of dimyristoylphosphatidylcholine into skin - Structural and spatial information from IR and Raman microscopic imaging, *Vib Spectrosc*, 38 (2005) 151-158.
- [8] P.J. Caspers, G.W. Lucassen, H.A. Bruining, G.J. Puppels, Automated depth-scanning confocal Raman microspectrometer for rapid in vivo determination of water concentration profiles in human skin, *J Raman Spectrosc*, 31 (2000) 813-818.
- [9] M. Melot, P.D.A. Pudney, A.M. Williamson, P.J. Caspers, A. Van Der Pol, G.J. Puppels, Studying the effectiveness of penetration enhancers to deliver retinol through the stratum corneum by in vivo confocal Raman spectroscopy, *J Control Release*, 138 (2009) 32-39.
- [10] J. Lademann, P.J. Caspers, A. van der Pol, H. Richter, A. Patzelt, L. Zastrow, M. Darwin, W. Sterry, J.W. Fluhr, In vivo Raman spectroscopy detects increased epidermal antioxidative potential with topically applied carotenoids, *Laser Phys Lett*, 6 (2009) 76-79.

- [11] G. Zhang, C.R. Flach, R. Mendelsohn, Tracking the dephosphorylation of resveratrol triphosphate in skin by confocal Raman microscopy, *J Control Release*, 123 (2007) 141-147.
- [12] A. Tfayli, O. Piot, F. Pitre, M. Manfait, Follow-up of drug permeation through excised human skin with confocal Raman microspectroscopy, *Eur Biophys J Biophys*, 36 (2007) 1049-1058.
- [13] C.H. Xiao, D.J. Moore, M.E. Rerek, C.R. Flach, R. Mendelsohn, Feasibility of tracking phospholipid permeation into skin using infrared and raman microscopic imaging, *J Invest Dermatol*, 124 (2005) 622-632.
- [14] N. Everall, Depth profiling with confocal Raman microscopy, part I, *Spectroscopy*, 19 (2004) 22-27.
- [15] N. Everall, Depth profiling with confocal Raman microscopy, part II, *Spectroscopy*, 19 (2004) 16-27.
- [16] C. Sourisseau, J.L. Bruneel, J.C. Lassegues, In-depth analyses by confocal Raman microspectrometry: experimental features and modeling of the refraction effects, *J Raman Spectrosc*, 33 (2002) 815-828.
- [17] O. Piot, A. Tfayli, M. Manfait, Confocal Raman microspectroscopy on excised human skin: uncertainties in depth profiling and mathematical correction applied to dermatological drug permeation, *J Biophotonics*, 1 (2008) 140-153.
- [18] M. Forster, M.A. Bolzinger, D. Ach, G. Montagnac, S. Briancon, Ingredients Tracking of Cosmetic Formulations in the Skin: A Confocal Raman Microscopy Investigation, *Pharm Res*, 28 (2011) 858-872.
- [19] E. Jaeckle, U.F. Schaefer, H. Loth, Comparison of effects of different ointment bases on the penetration of ketoprofen through heat-separated human epidermis and artificial lipid barriers, *J Pharm Sci-U.S.*, 92 (2003) 1396-1406.
- [20] S. Hansen, A. Henning, A. Naegel, M. Heisig, G. Wittum, D. Neumann, K.H. Kostka, J. Zbytovska, C.M. Lehr, U.F. Schaefer, In-silico model of skin penetration based on experimentally determined input parameters. Part I: Experimental determination of partition and diffusion coefficients, *Eur J Pharm Biopharm*, 68 (2008) 352-367.
- [21] A.M. Kligman, E. Christophel, Preparation of Isolated Sheets of Human Stratum Corneum, *Arch Dermatol*, 88 (1963) 702-705.
- [22] H.J. Yardley, R. Summerly, Lipid-Composition and Metabolism in Normal and Diseased Epidermis, *Pharmacol Therapeut*, 13 (1981) 357-383.

- [23] P.W. Wertz, D.C. Swartzendruber, K.C. Madison, D.T. Downing, Composition and Morphology of Epidermal Cyst Lipids, *J Invest Dermatol*, 89 (1987) 419-425.
- [24] B.C. Melnik, J. Hollmann, E. Erler, B. Verhoeven, G. Plewig, Microanalytical Screening of All Major Stratum-Corneum Lipids by Sequential High-Performance Thin-Layer Chromatography, *J Invest Dermatol*, 92 (1989) 231-234.
- [25] M.A. Lampe, A.L. Burlingame, J.A. Whitney, Human stratum corneum lipids: Characterization and regional variations, *J Lipid Res*, 24 (1983) 120-130.
- [26] S.M. Al-Saidan, B.W. Barry, A.C. Williams, Differential scanning calorimetry of human and animal stratum corneum membranes, *Int J Pharm*, 168 (1998) 17-22.
- [27] P.A. Cornwell, B.W. Barry, J.A. Bouwstra, G.S. Gooris, Modes of action of terpene penetration enhancers in human skin differential scanning calorimetry, small-angle X-ray diffraction and enhancer uptake studies, *Int J Pharm*, 127 (1996) 9-26.
- [28] M. Windbergs, C.J. Strachan, P. Kleinebudde, Investigating the Principles of Recrystallization from Glyceride Melts, *Aaps Pharmscitech*, 10 (2009) 1224-1233.
- [29] N. Garti, K. Sato, *Crystallization Processes in Fats and Lipid Systems* 1ed., CRC Press, 2001.
- [30] B.W. Barry, H.G.M. Edwards, A.C. Williams, Fourier-Transform Raman and Infrared Vibrational Study of Human Skin - Assignment of Spectral Bands, *J Raman Spectrosc*, 23 (1992) 641-645.
- [31] A. Knuttel, M. Boehlau-Godau, Spatially confined and temporally resolved refractive index and scattering evaluation in human skin performed with optical coherence tomography, *J Biomed Opt*, 5 (2000) 83-92.
- [32] M. Baranska, L.M. Proniewicz, Raman mapping of caffeine alkaloid, *Vib Spectrosc*, 48 (2008) 153-157.

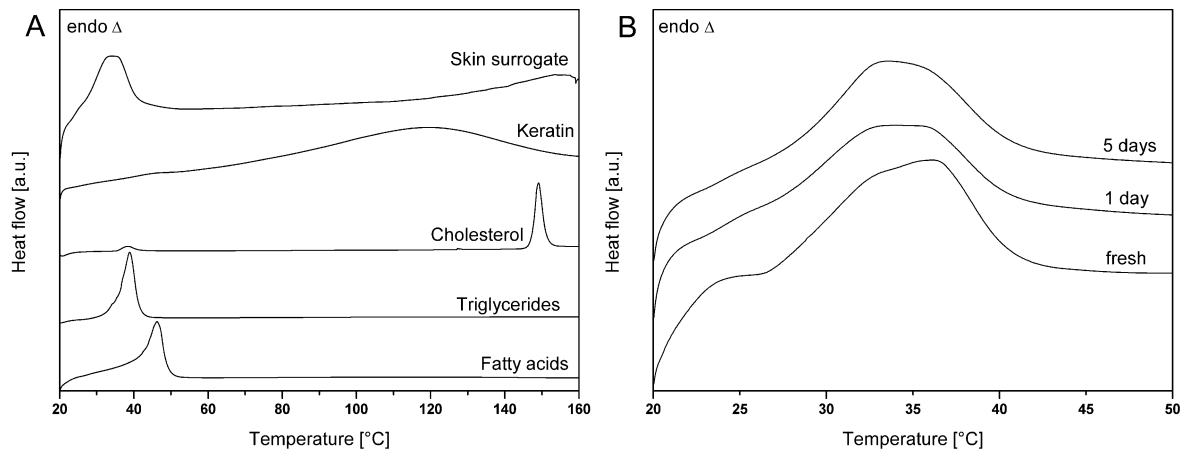


**Figure 1: Physical characterisation of the skin surrogate.**

DSC thermograms **A** comparison of skin surrogate and its single components **B** detail of the skin surrogate thermogram upon storage (mean,  $n = 3$ ).

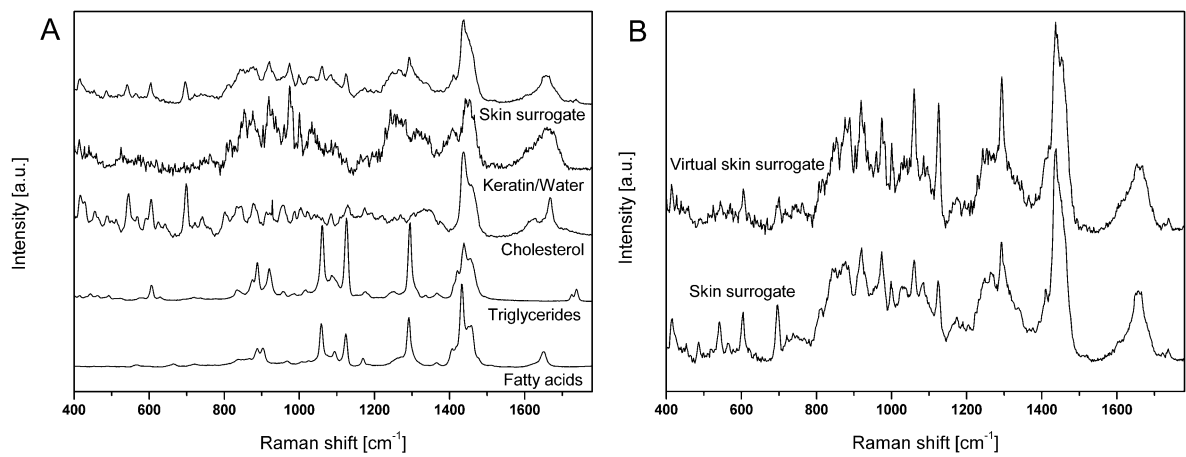


**Figure 2: Vibrational characterisation of the skin surrogate.**

Raman spectra **A** skin surrogate and its single components **B** comparison of virtual and real skin surrogate.

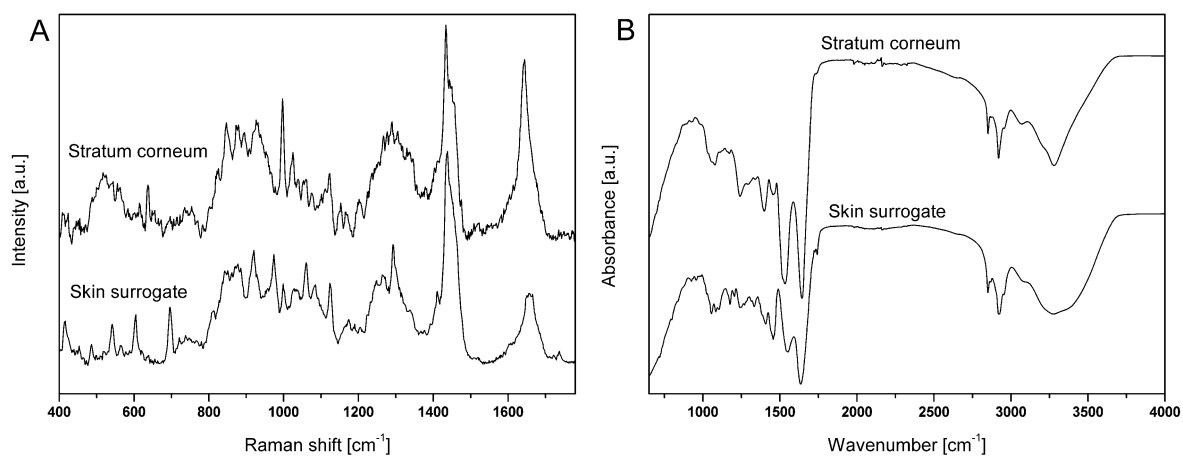


**Figure 3: Comparison of human stratum corneum and skin surrogate.**

**A** Raman spectra **B** IR spectra.

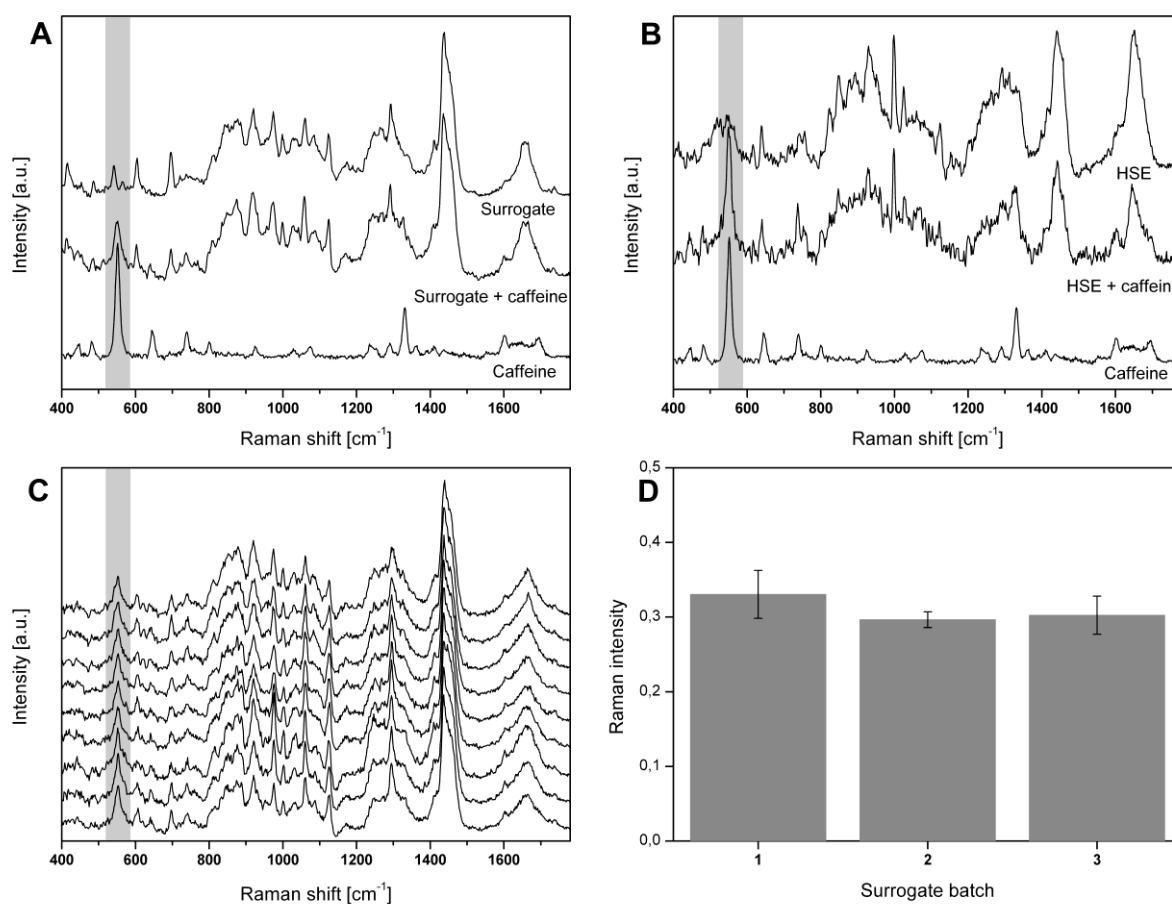


**Figure 4: Raman spectral evaluation of an incorporated model drug.**

Raman spectra of **A** skin surrogate, caffeine incorporated in skin surrogate and caffeine **B** HSE, HSE incubated with caffeine and caffeine **C** three different batches of skin surrogate with incorporated caffeine at three different positions. **D** caffeine representing peak intensities of three different surrogate batches (mean  $\pm$  SD, n = 6).

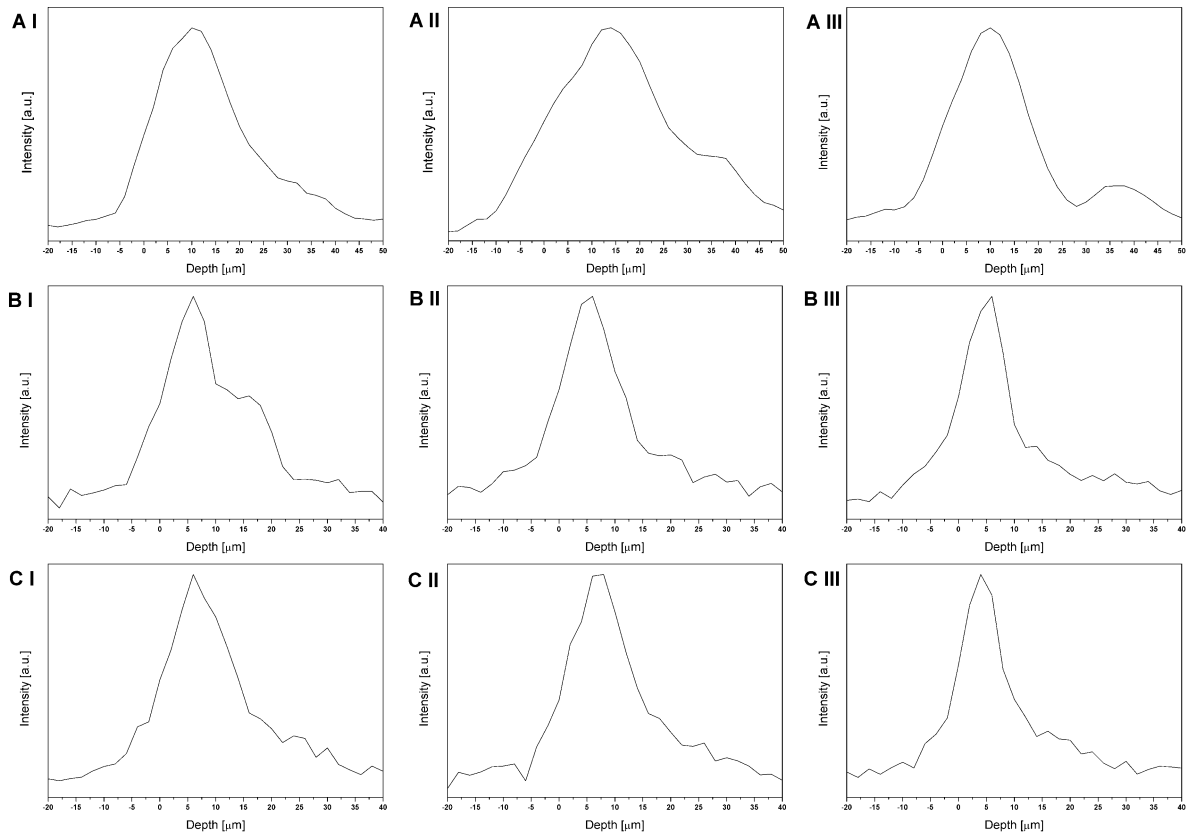


**Figure 5: Raman intensity depth profiles of caffeine.**

**A** three different batches of skin surrogate **B** and **C** heat separated epidermis of two different donors on three different positions.

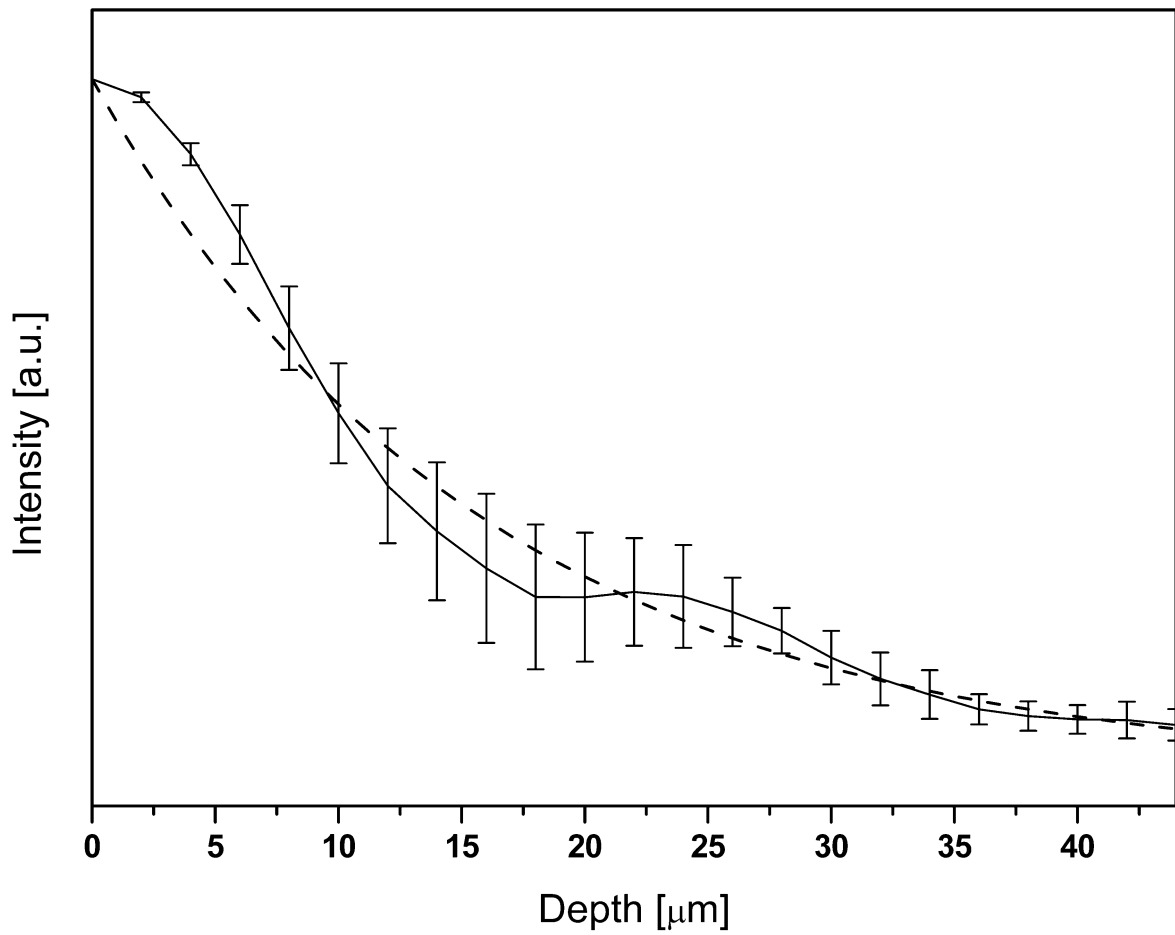


**Figure 6: Description of Raman signal attenuation.**

Raman mean drug intensity depth profile based on three skin surrogates (solid line mean  $\pm$  SD,  $n = 3$ ) and fitting function (dashed line).

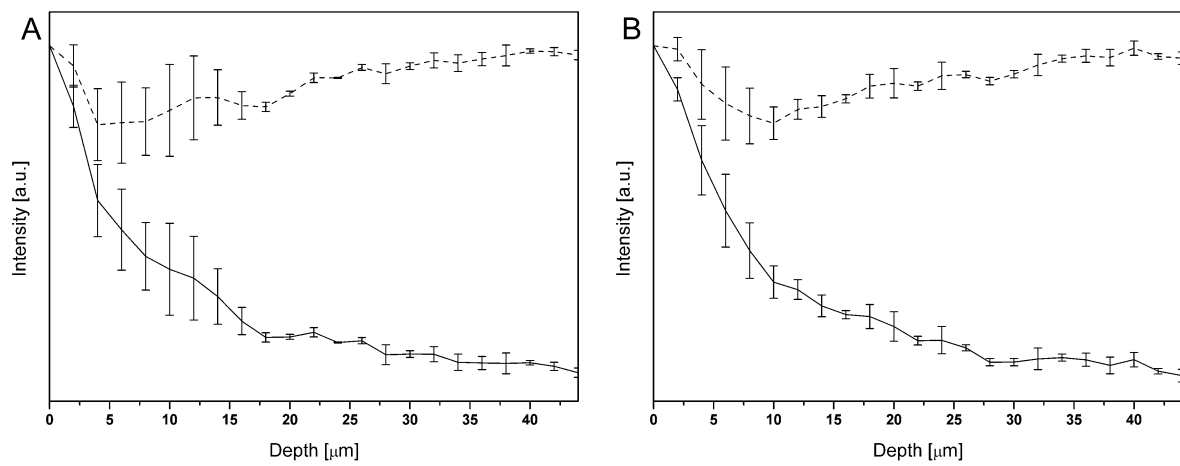


**Figure 7: Corrected Raman intensity depth profiles in human skin.**

**A** and **B** Raman mean intensity depth profile for caffeine in two skin donors (solid line, mean ± SD, n = 3) and corrected profile (dashed line, mean ± SD, n = 3).

<b>Ingredients</b>	<b>Skin surrogate composition (w/w) [%]</b>
Keratin	42
Water	28
Lipids	30
└ Cholesterol	└ 9.3
└ Triglycerides	└ 9.3
└ Fatty acids	└ 11.4
└ Myristic acid	└ 0.27
└ Palmitic acid	└ 4.35
└ Stearic acid	└ 1.23
└ Oleic acid	└ 4.14
└ Linoleic acid	└ 1.41

**Table 1: Chemical composition of the skin surrogate.**

<b>Ingredients</b>	<b>Human stratum corneum composition (w/w) [%]</b>
Keratin	50-70
Water	10-40
Lipids	10-30
Fatty acids	9.1-26
Cholesterol	14-28.9
Triglycerides	0-25.2
Sterolesters	0.7-10
Ceramides	18.1-49.2
Other	1.9-18

**Table 2: Chemical composition of human stratum corneum [22-25].**